Vision Research 49 (2009) 2056–2066

Contents lists available at ScienceDirect

Vision Research

journal homepage: www.elsevier.com/locate/visres

# Summation characteristics of the detection of compound gratings

S. Plainis [a], N.R.A. Parry [b], A. Panorgias [c], P. Sapountzis [d], I.J. Murray [c,*]

[a] Institute of Vision and Optics (IVO), School of Health Sciences, University of Crete, Heraklion, Crete, Greece
[b] Vision Science Centre, Manchester Royal Eye Hospital, Manchester, UK
[c] Faculty of Life Sciences, Moffat Building, University of Manchester, P.O. Box 88, Manchester M60 1QD, UK
[d] Nottingham Visual Neuroscience, School of Psychology, University of Nottingham, Nottingham, UK

ARTICLE INFO

*Article history:*
Received 21 August 2008
Received in revised form 12 May 2009

*Keywords:*
Spatial frequency channels
Contrast
Compound gratings
Interactions
Probability summation

ABSTRACT

Many classical experiments have shown that two superimposed gratings are more easily detected than a single grating, in keeping with probability theory. Here we test the rules for the detection of 2-component compound gratings by extending the range of parameters used in previous experiments. Two complementary methods of deriving summation indices are described. Data are presented so that the conditions for the transition from probability to neural summation are easily identified. True probability summation occurs only when grating contrasts are carefully perceptually equalised and spatial frequency differs by more than a factor of 2. A wide range of contrast ratios of the component gratings were explored such that gratings were at different contrasts, relative to respective thresholds. We find clear evidence of suppressive interactions when the compound gratings are composed of a close to threshold low frequency component and a below-threshold higher spatial frequency component.



## 1. Introduction

The classic paper of Campbell and Robson (1968) tested the idea that the human visual system is composed of a spectrum of parallel linear filters, each tuned to different ranges of spatial frequencies. A fundamental prediction of this model is the orthogonality of spatial channels. Campbell and Robson (1968) approached this problem by comparing sensitivity to square and sine gratings. They found that, at threshold, observers detect only one of the Fourier components of square wave gratings. When spatial frequency is greater than around 4 c/deg, square wave gratings are detected more easily by a factor of $4/\pi$, as predicted by Fourier theory. Detectability of gratings below 4 c/deg is less predictable due to non-linearities, as discussed in Campbell and Robson (1968).

The existence and independence of spatial frequency channels was further supported by adaptation experiments (Blakemore & Campbell, 1969), by simultaneous masking (Carter & Henning, 1971) and by sub-threshold summation experiments (Graham & Nachmias, 1971). Most studies suggest that the individual channels have a spatial frequency bandwidth of about half to one octave at half maximum sensitivity, although this depends on the method of measurement and no study has conducted a systematic survey of the individual variations.

The notion of the so-called multiple-channel spatial frequency model generated much controversy and Klein (1991) provides a compelling perspective on the issues surrounding the bandwidth of the channels, their independence and their relationship to discrimination. Whether the bandwidths and centre-frequencies matched those expected from single unit physiology (Daugman, 1985; Field, 1987; Georgeson & Harris, 1984; Kulikowski, Marcelja, & Bishop, 1982; Sakitt & Barlow, 1982; Shapley & Lennie, 1985) and how the model might be developed to account for spatial position (Wilson & Gelb, 1984), orientation (Campbell, Kulikowski, & Levinson, 1966) and image size (Robson & Graham, 1981) have all been widely discussed. Understanding and characterising these mechanisms is obviously a fundamental problem for vision science. It is clear that their output culminates in form perception, in that they provide the basic building blocks for what Marr (1982) referred to as the primal sketch.

The usefulness and credibility of the more recent computationally intense models (Watson & Ahumada, 2005) relies on the clear exposition and understanding of the main empirical observations on which the modelling is based. One of the most influential observations in this respect is the detectability of two-component sinusoidal grating stimuli, otherwise known as compound gratings. The attraction of this class of stimuli is that they can be used to explicitly test the prediction of perceptual independence of the spatial frequency channels. The argument goes as follows: when two gratings are presented to an observer and added so that they are at their respective thresholds, provided they differ in spatial frequency by more than 2 octaves (the probable bandwidth of the

* Corresponding author.
*E-mail address:* Ian.j.murray@manchester.ac.uk (I.J. Murray).

0042-6989/$ - see front matter © 2009 Elsevier Ltd. All rights reserved.
doi:10.1016/j.visres.2009.05.006

hypothetical spatial frequency channels) they should be detected independently. That is, if the gratings are 4 and 16 c/deg, one channel will respond to 4 and not to 16 c/deg and the other channel will respond to 16 and not 4 c/deg. However, when they are superimposed, the resulting compound grating is more visible than when either is presented individually, due to probability summation. It has been proposed that contrast sensitivity to a compound grating is of the order of 20% (1.19×) better compared to the sensitivity of individual components (Laming, 1991a; Watson, 1982; Watson & Nachmias, 1980), under the assumption that noise is uncorrelated in the two channels.

The motivation for the present paper was to develop further the understanding of the visibility of compound gratings by extending the range of conditions under which they have been investigated previously. First, we wanted to extend the combinations of spatial frequencies. Previous work has mostly ignored the fact that the detection of different spatial frequencies is dominated by mechanisms having different temporal characteristics (Watson and Nachmias 1980 is a notable exception). For example, even when gratings are static, there is the possibility that movement detecting mechanisms, mediated by transient detectors, influence the detection of low spatial frequencies more than higher frequencies. Hence it might be thought, for example, that the combination or summation rules for a 1 c/deg and 4 c/deg compound grating might be different from those for a 4 c/deg and 16 c/deg compound grating. In order to avoid this issue the study was restricted to the descending linear branch of the contrast sensitivity function, using 4 c/deg as the lower (primary) component, the secondary component being multiples of this. This is important because of its implications for the underlying physiology; if the slightly lower thresholds are due to a passive process dictated only by probability theory, then this will apply regardless of the temporal characteristics of the underlying detecting mechanisms. On the other hand, if the underlying mechanisms are capable of some sort of non- linear, active additive process then different values of summation index might be obtained.

Second, we wanted to highlight the effects of testing a wide range of contrast ratios of the component gratings. Sub-threshold summation might be expected to influence the observations when one of the gratings is at threshold and the other is below its threshold. Following Graham and others, sensitivity to the compound grating is plotted in terms of contrast threshold, normalised with respect to the contrast threshold for the gratings presented individually (Robson & Graham, 1981). The method allows the computation of an index of summation at a single contrast ratio where the gratings are equally discriminable and detectable. The issue of discriminability is of particular importance here and is discussed in detail in King-Smith and Kulikowski (1975). Other contrast ratios, where the individual gratings in a pair are above or below their respective thresholds can also be plotted in this space so that sensitivity contours can be drawn and the possibility that detection is entirely probabilistic can be tested without relying on the assumption that the two gratings have been accurately equalised for detectability. A further advantage of this approach is that it allows the separation of mechanisms dominated by probability summation from those detecting the components in more complex ways, based perhaps on the local contrast of the individual stimuli.

In this paper we report the results of experiments which show how gratings interact when they are presented simultaneously. A wide range of spatial frequency pairs are tested and the data are presented in a novel way so that the borderline between neural and probability summation is unambiguous. In a second series of experiments we investigate the interaction effects obtained when grating pairs are presented simultaneously but at different contrasts relative to their thresholds.

## 2. Methods

The following notation is used in the manuscript:

$c_1$ = contrast for the primary grating,
$c_2$ = contrast for the secondary grating,
$\theta_1$ = contrast threshold for the primary grating,
$\theta_2$ = contrast threshold for the secondary grating,
$\theta_c$ = contrast threshold for the compound grating,
$f_1$ = spatial frequency of the primary grating,
$f_2$ = spatial frequency of the secondary grating,
$L_0$ = mean luminance.

Compound grating pairs were composed of a primary grating of spatial frequency $f_1$ = 4 c/deg, added to a secondary grating of spatial frequency $1.125f_1$, $1.25f_1$, $1.5f_1$, $2f_1$, $3f_1$, $4f_1$, $6f_1$. Hence stimuli were simple gratings of spatial frequency 4, 4.5, 5, 6, 8, 12, 16 and 24 c/deg or compound gratings composed of one of these added to 4 c/deg. The Michelson contrast ($C_M$) was defined as $C_M = (L_{MAX} - L_{MIN})/(L_{MAX} + L_{MIN})$ and expressed in dB. The sum of the two components forms a compound grating $S(x)$ which can be expressed as

$$S(x) = c_1 \sin(2\pi f_1 x) + c_2 \sin(2\pi f_2 x) \quad (1)$$

We can therefore express the luminance profile of the compound as follows

$$L(x) = L_0[1 + c_1 \sin(2\pi f_1 x) + c_2 \sin(2\pi f_2 x)] \quad (2)$$

as illustrated in Fig. 1.

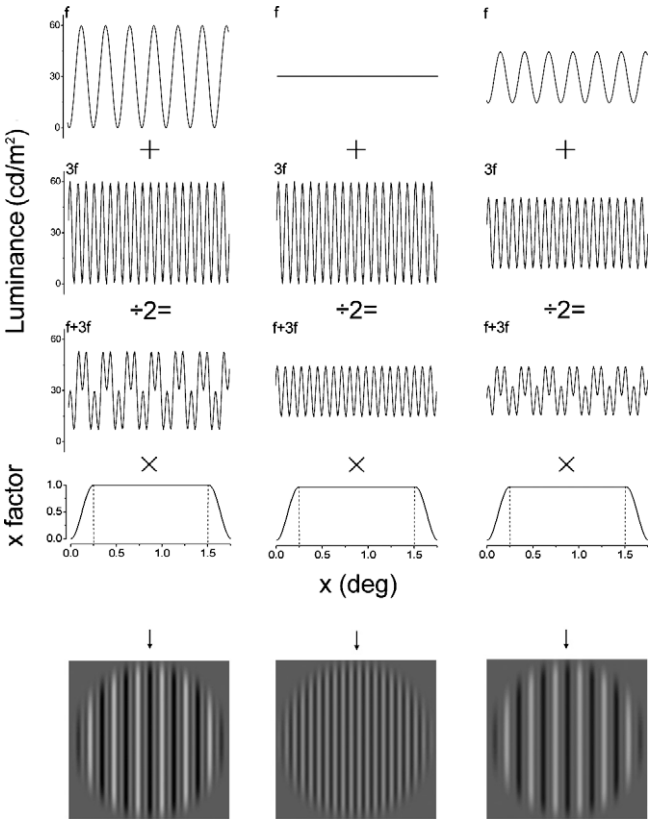


**Fig. 1.** Luminance profiles of a compound grating where the secondary grating was 3x the primary. The cosinusoidal profile is illustrated in the fourth row. The stimulus generated on the monitor is depicted in bottom row. Left Column: The contrasts of the two components are equal. Centre column: The contrast of the low spatial frequency component ($f$) is zero. Right column: The two components have different contrasts.

Single frequency and compound sinusoidal gratings were presented on a Sony GDM F-520 CRT display (frame rate 120 Hz) using a VSG2/5 stimulus generator card (CRS, Rochester, UK) and specially developed software. The grating patterns subtended 1.75°. The outer 0.25°, of the gratings was modulated with a circularly symmetrical raised cosinusoidal luminance profile to minimise edge effects (see Fig. 1). Stimuli were viewed monocularly at a distance of 3 m. There was a central fixation point, mean luminance was 30 cd/m$^2$ and the field size was 4.7° vertically and 5.9° horizontally.

In experiment one five observers were tested. All were experienced in setting thresholds. Their ages ranged from 27 to 54 and all were optically corrected to give normal visual acuity. In experiment two, two of the five observers were tested and the maximum spatial frequency was 16 c/deg instead of 24 c/deg.

### 2.1. Experiment 1. Grating pairs spanning 2.5 octaves

In the first experiment two conditions were tested. In the first, the contrast of the primary grating was set to zero so that only the secondary grating was detected. In the second condition, thresholds were obtained for the detection of the compound grating. Here the difference in contrast, $\Delta\theta$, between the two components remained constant so that

$$\Delta\theta = \theta_1 - \theta_2 \tag{3}$$

And so in this case Eq. (2) becomes

$$L(x) = L_0[1 + c_1 \sin(2\pi f_1 x) + [c_1 - \Delta\theta] \sin(2\pi f_2 x)] \tag{4}$$

This means that when setting thresholds for the detection of the compound grating, the components were yoked together so that the contrast difference between them remained constant and equal to $\Delta\theta$. This equalising procedure allowed us to test the critical condition when the combination of the gratings is expected, according to the standard theory, to show an improvement in sensitivity compared with that for one of the gratings alone.

### 2.2. Experiment 2. Grating pairs having different contrast ratios

In this experiment we explored the relationship between the sensitivity to the compound grating when either one or the other constituent grating was below its individual threshold. Under these conditions where either one or the other was more prominent, observers detected only one of the two gratings at threshold. Hence, following previous work (Graham, 1980; Logvinenko, 1993; Watson, 1982), as relative contrast is varied, we can then obtain a summation contour of the form:

$$[\theta_c/\theta_1]^{a1} + [\theta_c/\theta_2]^{a2} = 1 \tag{5}$$

In the curve fitting it is assumed that the summation contour is symmetrical about the $x$ and $y$ axis ($a1 = a2$) and so a single value for the exponent is obtained. The summation index for each contour is $2^{1/a}$. This means that in the case of complete one-to-one summation, the exponent $a$ would have a value of one, with the summation index being equal to two. On the other hand, in the absence of any summation, exponent $a$ would be $\infty$, with the summation index being equal to one. However, grating detectability is approximated by a fourth power transform (Foley & Legge, 1981; Laming, 1991b) i.e. $a = 4$. This results in probability summation for a two-component compound grating having a theoretical summation index of $2^{0.25} = 1.19$, as stated above. Note that for a stimulus composed of three component gratings the advantage according to probability would be $3^{0.25} = 1.31$ and so on.

## 3. Results

### 3.1. Experiment 1. Grating pairs spanning 2.5 octaves

In Fig. 2 we present the data from the first series of experiments for five observers. In a single session, thresholds for two conditions, $c_1 = 0$ (contrast of primary grating is set to 0) and $c_2 = c_1 - \Delta\theta$, in which the contrast of the two gratings is equalised with respect to their respective thresholds, were obtained for each grating pair. Contrast sensitivity (CS) is plotted in dB, i.e.

$$\mathrm{CS}_{db} = 20 * \log_{10}(1/\theta). \tag{6}$$

The first horizontal axis indicates frequency ratio, $r$, of the grating pairs ranging from 1 to 6, that is over 2.5 octaves. The second (lower) horizontal axis shows the spatial frequency of the secondary grating. For the $c_1 = 0$ condition (open squares) sensitivity decreases as would be expected linearly with spatial frequency. Effectively, this is the sensitivity of the secondary grating alone. Sensitivity to the compound grating ($c_2 = c_1 - \Delta\theta$) is plotted as open circles for each spatial frequency pair. Note that the objective of these experiments was to determine the extent to which the detectability of the compound was increased compared with that of a single grating. We therefore plot the difference between these two functions for each pair of frequencies in the lower panel as open circles.

In Fig. 3 the sensitivity-difference plots and their means for all observers are illustrated. The left hand axis is the increase in sensitivity in dB for the compound gratings compared with that of the secondary grating alone. The right hand axis is the equivalent threshold ratio. The upper horizontal axis indicates the spatial frequency of the secondary grating and the lower is spatial frequency in octaves of the secondary grating compared with the primary. Each observer is represented by an open circle. We can assume the peak of this function to be at 6 dB. That is, there is a (2×) increase in sensitivity to the compound compared with that for the individual gratings when the gratings are the same or similar (e.g. 4.5 c/deg) spatial frequencies.

For the special case, when the secondary grating is 8 c/deg the two components are exactly in phase and there is a systematic increase in relative sensitivity for all observers. Here, there is inevitably an improvement in sensitivity because the peaks and troughs of the luminance profile add and subtract. As outlined below (Section 4) Graham (1980) showed that the phase of the constituent gratings did not affect detectability of the compound. However, when spatial frequency ratio is exactly 2, phase may have an impact. As the difference in spatial frequency increases, sensitivity levels off to a plateau which is close to the theoretical value of 2 dB (1.25×), consistent with probability summation. The dashed line is a least squares best-fit Lorentzian function through the means as follows

$$P(x) = y_0 + (y_c - y_0)\frac{w^2}{4(x - x_0^2 + w^2)} \tag{7}$$

where $w$ is the Full Width at Half Maximum (FWHM), $x_0$ = Centre (4 c/deg), $y_c$ = Peak (6 dB) and $y_0$ = asymptote.

As discussed in many previous papers (Watson, 1982), this function illustrates the critical spatial frequency pair where neural summation ceases and only probability summation remains. It may therefore be regarded as one half of a spatial frequency tuning function with a peak at 4 c/deg. Assuming the peak of this function is at 6 dB, that it is symmetrical, and the minimum is at the theoretical limit of 2 dB, the bandwidth at FWHM of the complete tuning function will be 0.30 octaves according to Eq. (7). This is very close to the value obtained by Watson (1982), using compound gratings and a method similar to our experiment 2 (see below), of between 0.25 and 0.5 octaves for a single observer. The

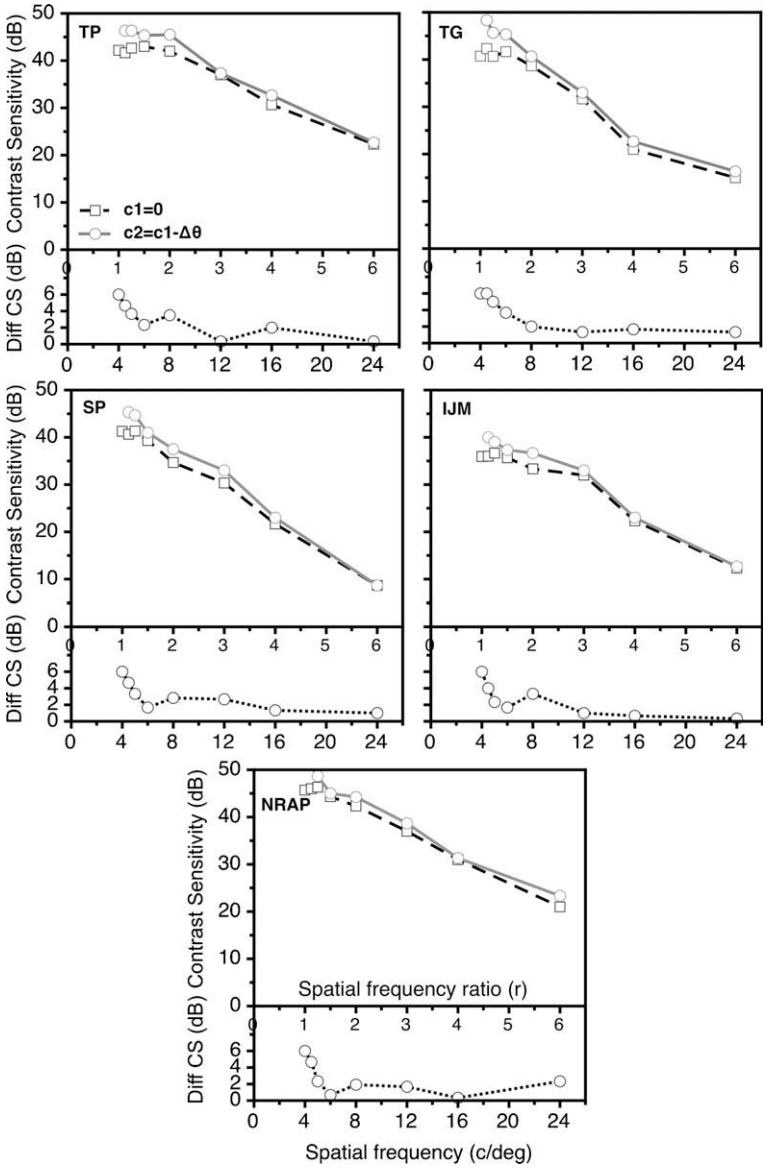


**Fig. 2.** Contrast sensitivity for a series of compound gratings for five subjects. The spatial frequency of the primary component was 4 c/deg in all cases. The spatial frequency of the secondary, higher spatial frequency component, ranged between 4.5 and 24 c/deg. The spatial frequency ratios, r, varied from 1.125 to 6.0 and these are depicted in the upper of the two *x* axis.

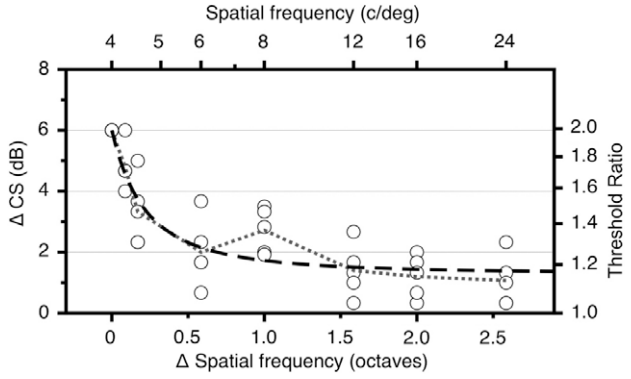


**Fig. 3.** Plots of the difference in contrast sensitivity (left axis) between $c_1 = 0$ and $c_2 = c1 - \Delta\theta$ for all subjects, derived from Fig. 2. The right axis is threshold ratio. The dotted line corresponds to the average values. The dashed line is a best-fitted Lorentzian function. Note that true probability summation occurs at 3× (1.8 octaves) the primary spatial frequency.

advantage of the Lorentzian, over an exponential function, which was used by Watson (1982), is that it has longer tails. Regardless of how the data are fitted, it is obvious that when the two gratings are similar, they have relatively high summation indices, that is additive mechanisms are operating. When they are 1.8 octaves (i.e. 3×) or more apart, there is no neural summation and they are detected by independent mechanisms.

### 3.2. Experiment 2. Gratings pairs having different contrasts

In this section we describe a different technique for obtaining summation indices for the compound gratings, namely by determining thresholds for a wide range of relative contrasts of the two gratings. In Fig. 4, summation contours are plotted for observers SP (Fig. 4a) and TP (Fig. 4b) for compound gratings with different spatial frequency pairs. In each panel, the spatial frequencies are indicated in the top right corner. Where two trials were conducted these are indicated by open and filled circles. The data depict the normalised sensitivity with respect to sensitivity to the

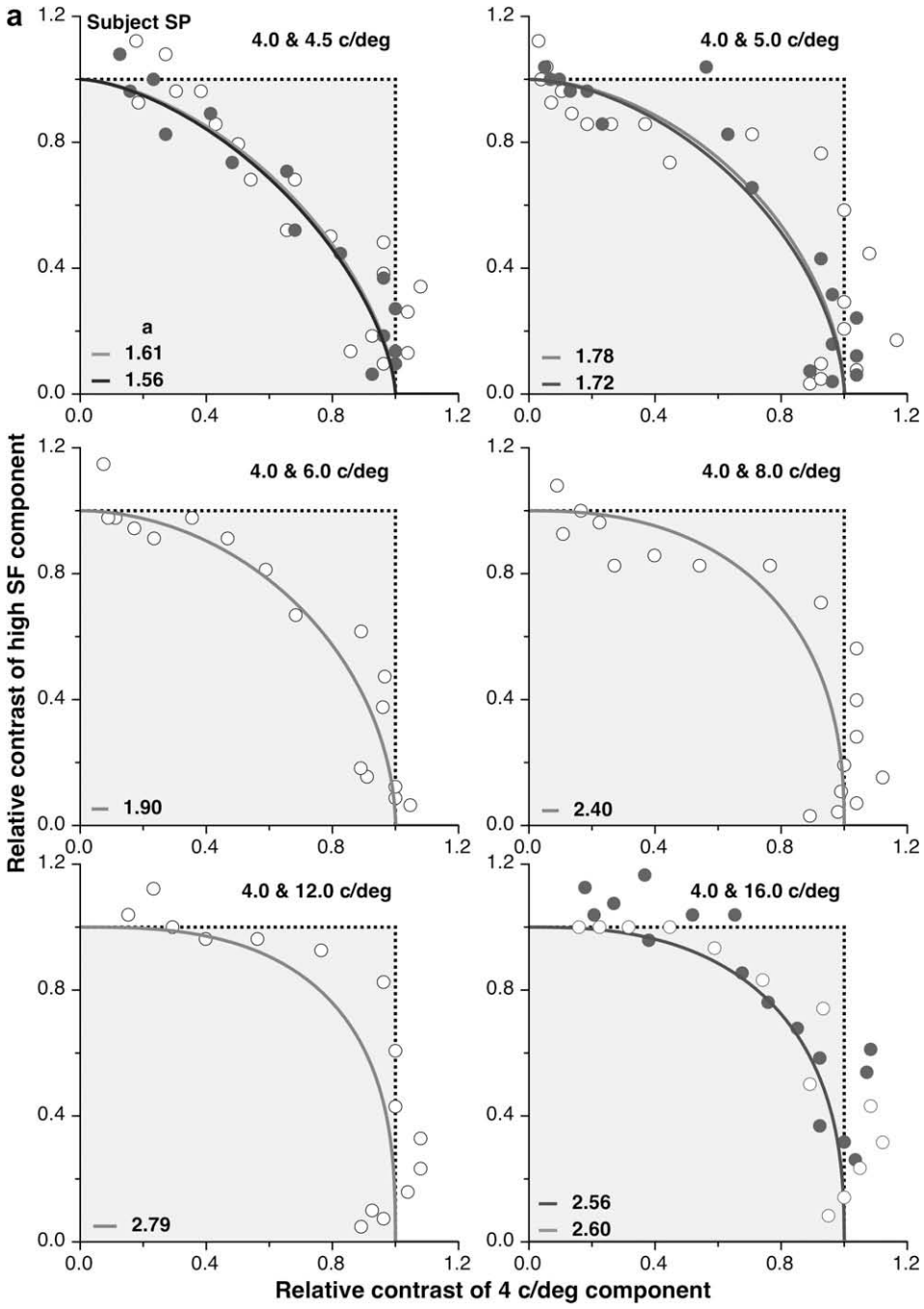


**Fig. 4.** The contrasts of the two components normalised with respect to their respective threshold for a series of compound grating pairs for subjects SP (a) and TP (b). Data were fitted using Eq. (5). Data were excluded from the fit if $x$ or $y$ was higher than 1. The two best-fitted curves correspond to two runs. The values for exponent $a$ are indicated at the bottom right of each panel.

individual grating presented alone and are similar to many other summation contours described in the literature e.g. Graham and Nachmias (1971). Each data point represents sensitivity to the compound grating obtained for a particular relative contrast. These span a sufficiently wide range so that in the extremes, only one or the other of the two gratings is visible at threshold. For example, where data points lie along the horizontal dotted line the observer sets threshold only to the grating with the higher spatial frequency because the primary grating is well below its threshold. Where the data lie along the vertical dotted line, the reverse applies and only the primary grating is detected. Intermediate data points have been fitted using Eq. (5), under the assumption that a probability summation model accounts for the condition where the two gratings are equally visible at threshold and that $a1 = a2$, i.e. that the data are symmetrically distributed within the constraints of the model. The values for exponent $a$ are indicated in each panel. Data are necessarily excluded from the fit when $x$ or $y$ is >1, according to Eq. (5). Note that data points outside the unit square represent suppressive interactions and those inside the unit square represent additive interactions.

The top left panel (4 + 4.5 c/deg, $r = 1.125$) illustrates a condition where neural summation would be expected between the gratings because they are likely to be detected by a single channel. For observer TP (Fig. 4b) there is almost perfect summation

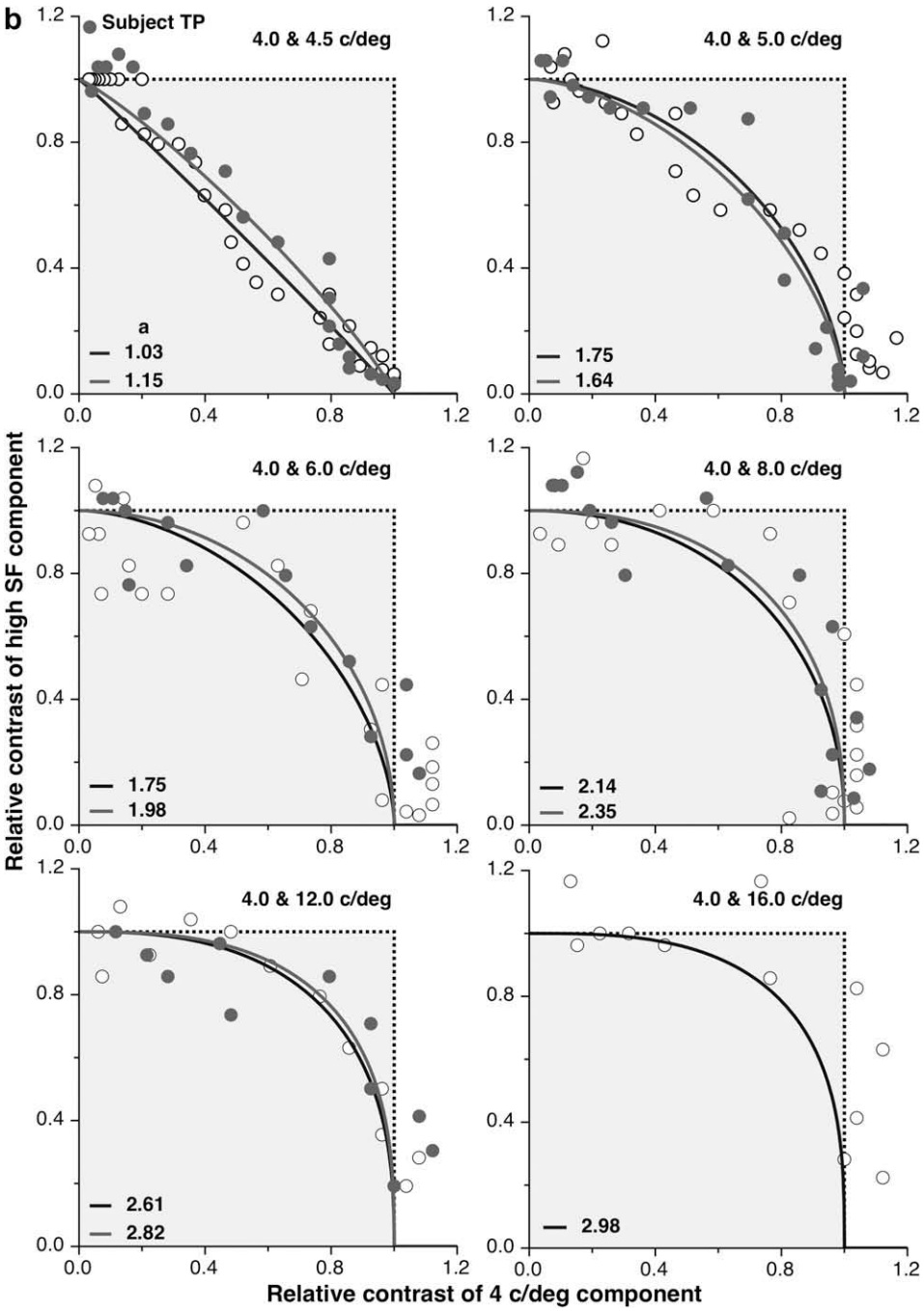


**Fig. 4** (*continued*)

($a$ = 1.03 for trial 1 and 1.15 for trial 2) whereas for SP, $a$ = 1.61 for one trial and 1.56 for the other. Apart from this grating pair, there are minimal differences between the two observers. For 4 + 5 c/deg, there would be more summation than expected due to probabilistic detection by independent channels and values of $a$ lie between 1.64 and 1.78 for the two observers. It is clear that $a$ increases (and detectability decreases) as the separation between gratings increases so that, for 4 + 12 c/deg, summation is largely probabilistic with $a$ being greater than 2.

Fig. 5 summarises the data in Fig. 4a and 4b for observers SP and TP. The high spatial frequency component of the grating pair is indicated in the left panel. We present these data to illustrate that there are only qualitative differences between these two observers. For example, in both subjects there is a similar gap between $r$ = 2 ($f$ = 8 c/deg) and $r$ = 1.5 ($f$ = 6 c/deg). Note that the differences between these observers, though slight, will manifest as different spatial frequency bandwidths.

In Fig. 6, threshold ratios from the summation contours in Figs. 4 and 5 are derived. The left vertical axis is threshold ratio and the right vertical axis is threshold difference in dB. As in Fig. 3, complete (neural) summation between the two components corresponds to a summation index of two (6 dB). Probability summation alone would give a value of between 1 and 2 dB which is around 1.2× (Watson & Nachmias, 1980), and this is very close to what we have found. The dashed lines are best-fit Lorentzian functions. Again, as in Fig. 3, these can be regarded as one half of a spatial frequency tuning function. The bandwidth at FWHM of a complete tuning function was calculated from Eq. (7), to be 0.24

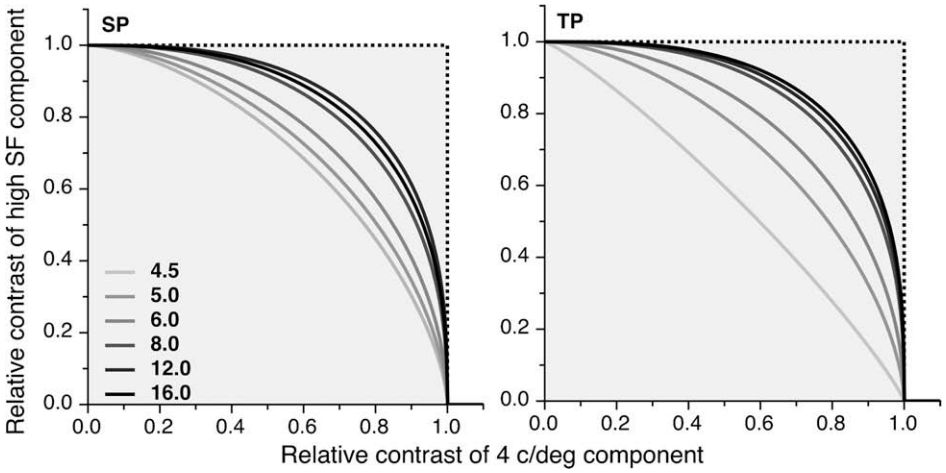


**Fig. 5.** A summary of the curves fitted in Fig. 4 for both subjects. Plots of the relative contrasts of the two components. The first component has a spatial frequency of 4 c/deg, while the higher spatial frequency component ranged between 4.5 and 16 c/deg.

octaves for SP and 0.58 octaves for TP. It is evident that this alternative approach to the determination of the summation index yields compatible data to that obtained from the five observers shown in Fig. 3.

A limitation with this analysis is that the curve fitting in Figs. 4a and b assumes the gratings interact symmetrically. That is $a_1 = a_2$ in Eq. (5). For $a_1 \neq a_2$ the curve would not be symmetrical about the $x$ and $y$ axes. The data in Fig. 6 suggest that this assumption

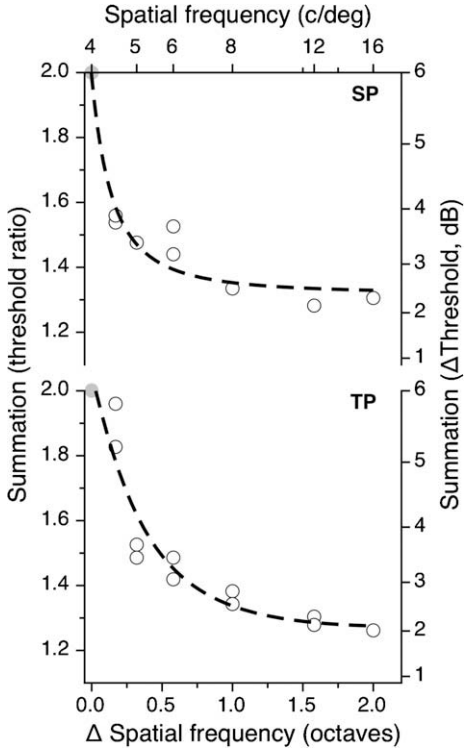


**Fig. 6.** Plots of the summation index expressed in threshold ratio (left axis) and summation in terms of dBs (right axis) as a function of the spatial frequency difference in octaves between the secondary and the primary components. Data from subjects SP (upper graph) and TP (lower graph) are presented. Complete summation between the two components corresponds to a value of 2, while probability summation would give a ratio of 1.2. The dashed lines are best-fitted Lorentzian functions.

of symmetry may not hold. Any departure from symmetry in the summation curve is important because it implies that there are different interactions between the gratings when they are either below or above their respective thresholds and that these interaction vary depending on frequency pair.

To investigate these interaction effects and to clarify the interpretation of the sensitivity contours, the data from Fig. 4 are replotted in Fig. 7, as follows. The $x$ axis is the amount by which the secondary grating changed above or below the equalised contrast *point* for the grating pairs. Hence, when this is zero, the two gratings are equalised according to their difference in sensitivity. When $x$ is positive the higher spatial frequency (secondary grating) is predominant and when $x$ is negative, the lower spatial frequency (primary grating) is predominant. The vertical axis shows the difference in sensitivity between the compound grating and its individual components, i.e. $\theta_c - \theta_1$ and $\theta_c - \theta_2$. As in Fig. 3, 6dB represents complete summation.

Five spatial frequency pairs for two subjects, SP and TP, are illustrated. The top panel depicts a compound composed of 4 and 4.5 c/deg gratings. These spatial frequencies can be expected to summate neurally because they are within a spatial frequency channel. Less summation is found for the 4 and 5 c/deg pair. The three lower panels illustrate spatial frequency pairs that, according to the standard theory, are detected by independent mechanisms.

In the case of the upper panels where linear interaction between grating pairs occurs, sensitivity to the compound is improved by around 6 dB compared with either of the individual gratings when $x = 0$. Here, the gratings are equalised with respect to their respective thresholds. In the lower panels, where spatial frequency pairs differ by more than 2×, the patterns are expected to be detected independently, according only to probability theory. For these conditions and when $x = 0$, the presence of the second grating should confer only marginal advantage compared with the individual grating of around 1–2 dB, and this is the case.

However, inspection of the lower three panels reveals that the functions describing detection when the primary grating dominates detection of the compound, are quite different from those when the secondary grating predominates. As the relative contrast of the secondary grating is increased, sensitivity to the compound decreases, approximately linearly. When relative contrast of the primary grating increases, (note the reverse scale) sensitivity to the compound is reduced, in some cases below zero indicating the presence of suppressive interactions. There are obvious asymmetries in the action of the primary and secondary gratings when

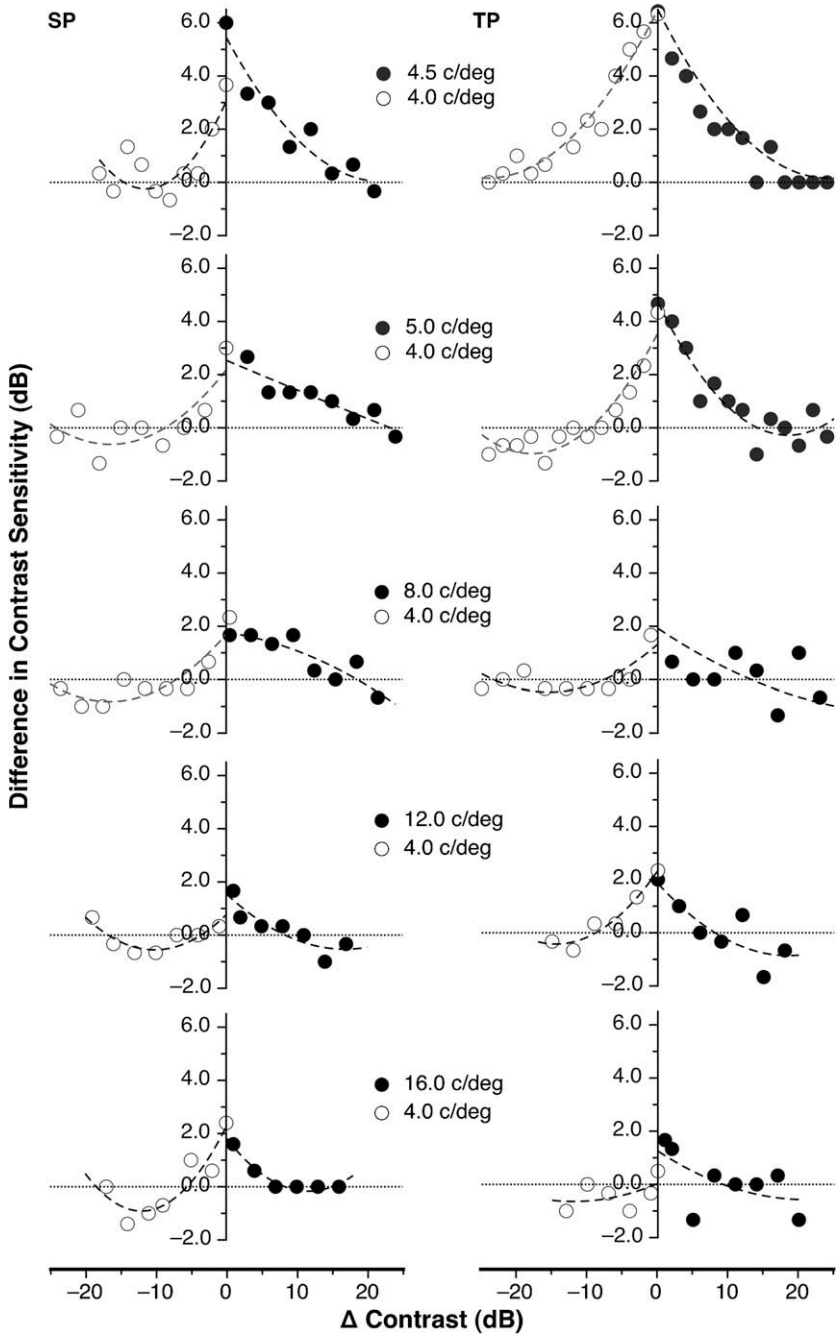


**Fig. 7.** The contrast sensitivity difference between the compound and individual gratings ($\theta_c - \theta_2$ or $\theta_c - \theta_1$) for a range of contrast differences between the components. The *x* axis is the amount by which the secondary grating was changed above or below the equalised contrast *point* for the grating pairs. When this is zero, the two gratings are equally visible, that is equalised according to their difference in sensitivity. The negative values indicate conditions where mainly the low spatial frequency is detectable at threshold and the positive values conditions where mainly the higher spatial frequency is detectable at threshold. The dashed lines are second order polynomial fits.

they are above their respective thresholds in the compound. These effects are also evident in the data of Fig. 4 at the extremes of the *x* axis which indicates the relative contrast of the 4 c/deg component ($\theta_c/\theta_1$) condition. There are more data points outside of the unity line here than there are in the corresponding extremes of $\theta_c/\theta_2$, relative contrast of the secondary grating. These interactions are discussed further below.

## 4. Discussion

The data presented confirm previous observations about the detectability of compound gratings. Provided they are at least 2× apart, the sum of two gratings is approximately 20% (1.2×) more detectable than the individual components. This improvement in sensitivity, though slight, is of major theoretical significance. It can be explained by probability summation as described by Sachs, Nachmias, and Robson (1971) and in detail by Graham (1980). Watson (1982) provides a succinct account of the effect. The empirical values obtained for the advantage of a 2-component grating over a single-component grating vary markedly in the literature. One of the main objectives of the present study was to clarify the issue by obtaining summation indices for a wide range of stimulus parameters and for different observers. We are therefore able to establish a simple perspective on acceptable values for the effect

and to provide an indication of individual variability. Figs. 3 and 6 suggest that in order to account for small individual variations, detection based solely on probability does not occur until 12 c/deg in our experiments. A good rule of thumb might be 3× or, as stated above, 1.8 octaves.

Watson (1982) showed, for an example compound grating, a range of summation contours whose exponents ($a$) were between 2.1 and 5.95. These give threshold ratio of 1.35 and 1.12, respectively. Using two approaches of deriving the index (see Figs. 2 and 4) our threshold ratios are close to the theoretical value of 1.19 as discussed in Watson and Nachmias (1980) and Laming (1991a). Note, however, that this theoretical value is founded on the assumption that the detectability function for a single grating approximates a fourth power transform of contrast. As discussed in elaborate detail in Laming (1991b), this depends on the model used for describing the properties of grating detection, but is fairly close to the value obtained experimentally. As outlined in Section 2, the relationship between the exponent $a$ in Eq. (5) and the summation rule ($2^{1/a}$) for 2-component gratings is itself exponential, so extremes of $a$ (2.14–2.98 in our case) do not affect the generality of the observations very much.

At extreme values of the contrast ratio there are distinct interaction effects which are not seen when the gratings are equally discriminable and detectable. They are also not particularly obvious in Fig. 4, where they appear to be random noise. This interesting finding has both practical and theoretical implications for the understanding of how the visual system processes multi-spatial frequency stimuli. Practically, it means that different values of summation index will be obtained if the gratings are not set to be precisely equally detectable before they are combined. From a theoretical point of view, it suggests that the bandwidths of the spatial frequency channels change with contrast and of course this is not surprising. This point has received lots of coverage in the literature because there is a very wide range of bandwidths represented in the visual cortex (Kulikowski et al., 1982).

As discussed in Klein (1991), psychophysical models rarely consider multi-bandwidth systems because this would limit their predictive ability. Some argue that, such is the complexity of the most simple cortical units, responding simultaneously to a myriad spatial frequencies, orientations and contrast that modelling, though theoretically valuable, has many practical limitations (Watson & Ahumada, 2005). Nevertheless the consensus seems to be that either a Gabor or a Lorentzian function, though limited, is the most acceptable weighting function for the receptive fields of simple cells in visual cortex; it minimises uncertainty between space and spatial frequency, provides information about a broad range of frequencies over a small spatial window, and has physiologically meaningful parameters.

The interactions described here are spatial frequency dependent and can be seen in Fig. 3 of Graham and Nachmias (1971). They are evident in the summation contours in our Fig. 4 in that, at the extremes of the $x$ and $y$ axes, data points appear to cluster outside the unit square when the lower spatial frequency predominates and inside the unit square when the higher spatial frequency predominates. The summation contours are not easy to interpret, partly because the relative contrast scale exaggerates small changes in contrast sensitivity, and partly because they appear to be rather noisy despite well planned methodology. When the data are re-plotted as in Fig. 7 their significance is immediately apparent. The suppressive interactions are actually quite systematic.

When the component gratings are detected by the same channel, for example 4 and 4.5 c/deg, there is neural summation and the compound is detected almost 2× (6 dB) better than either of the components alone. For spatial frequency ratios >2 the detectability of the compound is increased by a maximum of 2 dB compared with the individual grating, as predicted by probability summation. Note that there is a special case, in our experiments of 4 + 8 c/deg, where the mean luminance of the gratings match each other. This results in a small but conspicuous improvement in detectability (see Fig. 3) in all observers. King-Smith and Kulikowski (1975) claimed these conditions to be ideal for line and edge detectors and it may be that sensitivity is dictated more by local luminance effects rather than by spatial frequency detectors.

In most conditions an asymmetric pattern of interaction is observed. The reduction in the detectability of the compound is more pronounced as the contrast of the secondary grating is reduced below its threshold, i.e. the low spatial frequency dominates, than when the primary grating is presented below its threshold. Moreover, at spatial frequency ratios >2, when the contrast of the secondary grating is reduced below its threshold, sensitivity to the compound is less than zero before increasing at higher relative contrasts of the primary. The data points below zero are those showing suppressive interactions. Note that in Fig. 4 they appear outside of the unity square. There are no such inhibitory effects for the range of conditions where thresholds set only for the secondary grating and the primary grating is below its threshold. Here sensitivity to the compound is gradually reduced.

This may be related to the relative gains of the underlying detecting mechanisms. Similar effects using a detection and discrimination paradigm were described by Olzak (1985). She also found apparent inhibitory effects and these were asymmetric in the same way as illustrated in Fig. 7. That is, the presence of a (sub-threshold) high frequency grating reduces the response to the compound grating, but the reverse does not apply, i.e. the presence of a sub-threshold low frequency grating does not affect the detection of the compound grating.

Whether or not these represent true violations of the independent spatial channels hypothesis depends on which underlying assumptions are adopted for the modelling and how the data are interpreted. Klein (1991, 1985) has highlighted the dangers of assuming that channels are interacting. He regarded the interactions in the discrimination data described in Olzak (1985) as due to a combination of response bias and correlated noise. Of course, if the bandwidth of the channels increases with contrast then correlated noise will be present in the responses whenever contrast of either of the two gratings exceeds its threshold. This does not, however, explain why the interactions are asymmetric.

Regardless of whether or not the effects seen in Fig. 7 are theoretically significant, it is important to point out that they highlight a limitation to the interpretation of the summation contours and clarify their interpretation. Eq. (5) is fitted to the data assuming the two exponents $a_1$ and $a_2$ are equal. We have found that the fit can be improved by allowing these to vary, but, before adopting this strategy, it is important to establish the rules controlling the detection of pairs of gratings for a range of contrasts where either the low or high spatial frequency is detected at threshold for the compound. These experiments are in progress at present and will be reported in a separate paper.

There is some doubt about the extent of inhibitory interactions between putative spatial frequency analysers. As discussed briefly in Graham (1989) the issue revolves around the extent to which adaptation effects vary depending on the choice of paradigm. As elegantly described by Tolhurst (1972), inhibition does occur between channels but only at supra-threshold contrast. Klein and Stromeyer (1980) show that adaptation to a complex grating can not be due to inhibitory activity between channels.

It is important to note that the compound grating technique offers a relatively clean and rapid method of determining individual variations in spatial tuning bandwidth. As seen in Fig. 3, sensitivity improved rapidly as the difference in spatial frequency of the two gratings in a compound reduced, that is when neural (as opposed to probabilistic) interactions occur.

A final point concerns the bandwidth of the channels revealed with compound gratings. Our data suggest quite narrow tuning compared, for example, with Blakemore and Campbell (1969) who used adaptation and electrophysiological paradigms to obtain a value of a little more than one octave. As revealed by the single-unit studies, there is a wide array of bandwidths in the macaque visual cortex from 0.5 to 4 octaves (Xing, Ringach, Shapley, & Hawken, 2004). Bandwidth certainly varies with contrast, and the data presented here might be expected to indicate particularly narrow tuning because all observations are made at, or close to threshold. Watson (1982) using compound gratings obtained bandwidths of 0.25 and 0.5 octaves, similar to those described here. In fact the new procedure (see Figs. 2 and 3) gives the same results and is much less time consuming.

## Acknowledgements

Sotiris Plainis is partly funded by the Regional Operational Programme of Crete and Greek General Secretariat for Research & Technology for the project titled "Visual performance and in-vehicle information systems". Neil Parry is supported by the Manchester Academic Health Sciences Centre (MAHSC) and the NIHR Manchester Biomedical Research Centre. Panagiotis Sapountzis and Athanasios Panorgias were MSc students of the multi-disciplinary course "Optics & Vision", University of Crete during this study.

## Appendix A

### A.1. Veiling luminance effect

If one of a grating pair is presented at zero contrast and the two gratings are of equal mean luminance, the resultant stimulus is a single grating whose physical contrast is reduced by a factor of 2 due to veiling luminance. Similarly we can predict that, if one of the gratings is substantially below its threshold then sensitivity to the combination is again reduced by a factor of two. This idea is illustrated in Fig. 8 which illustrates the results of a control experiment in which the physical contrast of the primary and secondary grating were equal ($c_1 = c_2$). As the difference in spatial frequency between the two gratings increases, the secondary spatial frequency contributes less to the detectability of the compound. At a critical value (here $r < 2$), sensitivity to the compound reaches a plateau because the secondary grating is below its threshold. Here the observer detects the 4 c/deg grating on its own, apart from the veiling effect of the secondary grating, which, as outlined below is a reduction in physical contrast by 6 dB (2×) when the two gratings have equal mean luminance $L_o$.

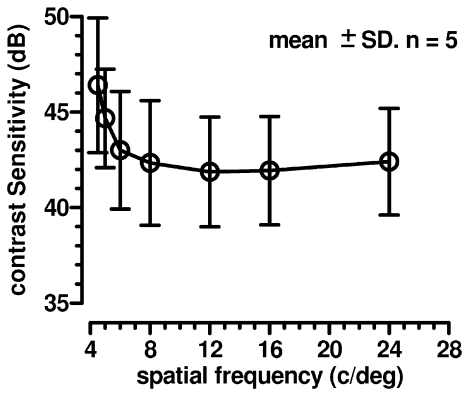


**Fig. 8.** Contrast sensitivity for condition $c_1 = c_2$. The component gratings are at equal physical contrast. Note that when sensitivity to the higher spatial frequency is reduced there is a 2× decrease in sensitivity, due to veiling luminance.

If we take contrast as defined by Michaelson to be as follows:

$$C = \frac{L_{max} - L_{min}}{L_{max} + L_{min}} \quad (A)$$

where $C$ is the contrast, $L_{max}$ the maximum luminance, $L_{min}$ the minimum luminance and veiling luminance is the $L_v$ resulting in reduced contrast, C′, then

$$C' = \frac{(L_{max} + L_v - (L_{min} + L_v))}{(L_{max} + L_v) + (L_{min} + l_v)} = \frac{L_{max} - L_{min}}{(L_{max} + L_{min}) + 2L_v} \quad (B)$$

$$\text{but } L_{max} + L_{min} = 2L_o \quad (C)$$

substituting in (B)

$$\text{gives } C' = \frac{L_{max} - L_{min}}{2L_o + 2L_v} \quad (D)$$

$$\text{Hence, contrast attenuating factor } C_a = \frac{C'}{C} \quad (E)$$

and

$$C_a = \frac{L_{max} + L_{min}}{L_{max} - l_{min}} \frac{L_{max} - L_{min}}{2L_o + 2L_v} = \frac{2L_o}{2L_o + 2L_v} = \frac{L_o}{L_o + L_v} \quad (F)$$

For the special case of $L_o = L_v$ contrast is reduced by 2×.

## References

Blakemore, C., & Campbell, F. W. (1969). On the existence of neurones in the human visual system selectively sensitive to the orientation and size of retinal images. *Journal of Physiology, 203*(1), 237–260.
Campbell, F. W., Kulikowski, J. J., & Levinson, J. (1966). The effect of orientation on the visual resolution of gratings. *Journal of Physiology, 187*(2), 427–436.
Campbell, F. W., & Robson, J. G. (1968). Application of Fourier analysis to the visibility of gratings. *Journal of Physiology, 197*(3), 551–566.
Carter, B. E., & Henning, G. B. (1971). The detection of gratings in narrow-band visual noise. *Journal of Physiology, 219*(2), 355–365.
Daugman, J. G. (1985). Uncertainty relation for resolution in space, spatial frequency, and orientation optimized by two-dimensional visual cortical filters. *Journal of the Optical Society of America A – Optics Image Science and Vision, 2*(7), 1160–1169.
Field, D. J. (1987). Relations between the statistics of natural images and the response properties of cortical cells. *Journal of the Optical Society of America A – Optics Image Science and Vision, 4*(12), 2379–2394.
Foley, J. M., & Legge, G. E. (1981). Contrast detection and near-threshold discrimination in human vision. *Vision Research, 21*(7), 1041–1053.
Georgeson, M. A., & Harris, M. G. (1984). Spatial selectivity of contrast adaptation: Models and data. *Vision Research, 24*(7), 729–741.
Graham, N. (1980). Spatial-frequency channels in human vision: Detecting edges without edge detectors. In C. S. Harris (Ed.), *Visual coding and adaptability* (pp. 225–262). Hillsdale, NJ: Lawrence Erlbraum Associates.
Graham, N., & Nachmias, J. (1971). Detection of grating patterns containing two spatial frequencies: A comparison of single-channel and multiple-channels models. *Vision Research, 11*(3), 251–259.
Graham, N. V. S. (1989). *Visual pattern analyzers. Oxford psychology series*. New York: Oxford University Press.
King-Smith, P. E., & Kulikowski, J. J. (1975). The detection of gratings by independent activation of line detectors. *Journal of Physiology, 247*(2), 237–271.
Klein, S. (1991). Channels: Bandwidth, channel independence, detection vs. discrimination. In B. Blum (Ed.), *Channels in the visual nervous system: Neurophysiology, psychophysics and models* (pp. 11–27). London and Tel Aviv: Freund.
Klein, S., & Stromeyer, C. F. III, (1980). On inhibition between spatial frequency channels: Adaptation to complex gratings. *Vision Research, 20*, 159–166.
Klein, S. A. (1985). Double-judgment psychophysics: Problems and solutions. *Journal of the Optical Society of America A – Optics Image Science and Vision, 2*(9), 1560–1585.
Kulikowski, J. J., Marcelja, S., & Bishop, P. O. (1982). Theory of spatial position and spatial frequency relations in the receptive fields of simple cells in the visual cortex. *Biological Cybernetics, 43*(3), 187–198.
Laming, D. (1991a). Spatial frequency channels. In J. J. Kulikowski, V. Walsh, & I. J. Murray (Eds.), *Limits of vision*. Basingstoke, Hants: Macmillan Press.
Laming, D. (1991b). Theoretical basis of the processing of simple visual stimuli. In J. J. Kulikowski, V. Walsh, & I. J. Murray (Eds.), *Limits of vision*. Basingstoke, Hants: Macmillan Press.

Logvinenko, A. D. (1993). Lack of convexity of threshold curves for compound gratings: Implications for modelling visual pattern detection. *Biological Cybernetics, 70*, 55–64.

Marr, D. (1982). *Vision: A computational investigation into the human representation and processing of visual information*. San Francisco: W.H. Freeman.

Olzak, L. A. (1985). Interactions between spatially tuned mechanisms: Converging evidence. *Journal of the Optical Society of America A – Optics Image Science and Vision, 2*(9), 1551–1559.

Robson, J. G., & Graham, N. (1981). Probability summation and regional variation in contrast sensitivity across the visual field. *Vision Research, 21*(3), 409–418.

Sachs, M. B., Nachmias, J., & Robson, J. G. (1971). Spatial-frequency channels in human vision. *Journal of the Optical Society of America A – Optics Image Science and Vision, 61*(9), 1176–1186.

Sakitt, B., & Barlow, H. B. (1982). A model for the economical encoding of the visual image in cerebral cortex. *Biological Cybernetics, 43*(2), 97–108.

Shapley, R., & Lennie, P. (1985). Spatial frequency analysis in the visual system. *Annual Review of Neuroscience, 8*, 547–583.

Tolhurst, D. J. (1972). Adaptation to square-wave gratings: Inhibition between spatial frequency channels in the human visual system. *Journal of Physiology, 226*, 231–248.

Watson, A. B. (1982). Summation of grating patches indicates many types of detector at one retinal location. *Vision Research, 22*(1), 17–25.

Watson, A. B., & Ahumada, A. J. Jr., (2005). A standard model for foveal detection of spatial contrast. *Journal of Visualization, 5*(9), 717–740.

Watson, A. B., & Nachmias, J. (1980). Summation of asynchronous gratings. *Vision Research, 20*(1), 91–94.

Wilson, H. R., & Gelb, D. J. (1984). Modified line-element theory for spatial-frequency and width discrimination. *Journal of the Optical Society of America A – Optics Image Science and Vision, 1*(1), 124–131.

Xing, D., Ringach, D. L., Shapley, R., & Hawken, M. J. (2004). Correlation of local and global orientation and spatial frequency tuning in macaque V1. *Journal of Physiology, 557*(Pt 3), 923–933.